Performance Analysis of Wideband Sum-of-Cisoids-Based Channel Simulators with Respect to the Bit Error Probability of DPSK OFDM Systems

Yuanyuan Ma and Matthias Pätzold
Faculty of Engineering and Science, University of Agder
P.O. Box 509, NO-4898 Grimstad, Norway
Email: {yuanyuan.ma, matthias.paetzold}@uia.no

Abstract—In this paper, we analyze the performance of a wideband sum-of-cisoids (SOC) channel simulator w.r.t. the bit error probability (BEP) of differential phase-shift keying (DPSK) orthogonal frequency division multiplexing (OFDM) systems. Analytical BEP expressions are derived for coherent and non-coherent DPSK OFDM simulation systems in the presence of a wideband SOC channel simulator. We also study the degradations of the BEP introduced by an imperfect channel simulator. Using the deviation of the BEP as an appropriate measure, we evaluate the performance of three parameter computation methods, known as the method of exact Doppler spread (MEDS), the randomized MEDS (R-MEDS), and the Monte Carlo method (MCM). For coherent DPSK OFDM systems, it turns out that these three methods are equivalent. For noncoherent DPSK OFDM systems, it is theoretically shown that both the MEDS and the R-MEDS outperform the MCM. The correctness of all theoretical results are validated by simulations.

I. INTRODUCTION

Rice's sum-of-sinusoids (SOS) principle has been accepted as a proper method for modeling mobile fading channels [1]–[3]. By applying the SOS principle combined with the concept of deterministic channel modeling [3], accurate and efficient SOS channel simulators can be easily designed for all kinds of channel models that can be derived from Gaussian random processes. Such channel simulators have been commonly used in system simulations due to their low realization expenditure. In recent years, the performance analysis of SOS channel simulators has been an important research subject. In [4], the performance of narrowband SOS channel simulators w.r.t. the BEP has been investigated.

The SOS method has been extensively employed in modeling flat fading channels [3], frequency-selective channels [3], and even wideband multiple-input multiple-output channels [5]. However, it has been shown in [6] that the SOS principle is of advantage for developing mobile radio channels in isotropic scattering environments, while in case of non-isotropic scattering environments, the SOC method is more efficient. So far, the performance of SOC channel simulators w.r.t. the BEP has not been studied. The purpose of this paper is to fill this gap.

In this paper, we study the performance of a DPSK OFDM system in the presence of a stochastic wideband SOC channel simulator w.r.t. the BEP of the simulation system. For comparison, we present the BEP of a DPSK OFDM system using a reference channel model, which is known as the reference BEP. As a starting point, we study the probability

density functions (PDFs) of the absolute value of the time-variant transfer function and the temporal-frequency correlation function (CF) of both channel models. Next, we derive the BEP expressions for the OFDM systems using coherent and noncoherent DPSK schemes. For the coherent DPSK OFDM system, we demonstrate that the BEP of the simulation system approaches to the reference BEP if the number of cisoids in the SOC channel simulator tends to infinity. Based on the analytical BEP results, we discuss the deviation between the reference BEP and the BEP of the simulation system. Then, we compare the performance of three parameter computation methods: the MEDS, the R-MEDS, and the MCM. We assume isotropic scattering conditions here. However, it should be mentioned that the obtained BEP expressions are general and also applicable to non-isotropic scattering conditions.

The rest of this paper is organized as follows. In Section II, we first give a brief review of the frequency-selective reference channel model and the corresponding SOC channel simulator. Then, we study the statistical properties of both channel models. Section III provides an analysis of the BEP performance of coherent DPSK OFDM systems. In Section IV, we concentrate on the noncoherent DPSK OFDM system performance analysis. Finally, the conclusions are given in Section VI.

II. FREQUENCY-SELECTIVE CHANNEL MODELS

In this section, a wide-sense stationary uncorrelated scattering (WSSUS) model [3], [7] is employed as an appropriate frequency-selective reference channel from which the SOC channel simulator is derived.

A. The Frequency-Selective Reference Channel Model

The time-variant transfer function of the wideband reference channel model can be formulated as [3]

$$H(f', t) = \sum_{\ell=1}^{\mathcal{L}} a_\ell \mu_\ell(t) e^{-j2\pi f' \tau'_\ell}, \qquad (1)$$

where $\mathcal{L}$ denotes the number of discrete propagation paths. The quantities a_ℓ and τ'_ℓ describe the path gain and the propagation delay of the ℓth discrete propagation path, respectively. The symbol $\mu_\ell(t)$ in (1) represents a complex random Gaussian process. It is supposed that the constraint $\sum_{\ell=1}^{\mathcal{L}} a_\ell^2 = 1$ holds to ensure that the average power of the channel model is normalized to unity. We assume that the real and imaginary

parts of $\mu_\ell(t)$ in (1) are uncorrelated Gaussian processes with zero-mean and the same variance $\sigma_0^2 = 1/2$.

Let $r_{HH}(v', \tau) = E\{H^*(f', t)H(f' + v', t + \tau)\}$ be the temporal-frequency CF of $H(f', t)$. According to [8], $r_{HH}(v', \tau)$ can be expressed in closed-form as

$$r_{HH}(v', \tau) = \sum_{\ell=1}^{\mathcal{L}} a_\ell^2 r_{\mu_\ell \mu_\ell}(\tau) e^{-j2\pi v' \tau_\ell'}, \quad (2)$$

where $r_{\mu_\ell \mu_\ell}(\tau)$ denotes the temporal autocorrelation function (ACF) of the Gaussian process $\mu_\ell(t)$. If we consider isotropic scattering conditions, the temporal ACF can be written as

$$r_{\mu_\ell \mu_\ell}(\tau) = 2\sigma_0^2 J_0(2\pi f_{\max} \tau), \quad (3)$$

where $J(\cdot)$ represents the zeroth-order Bessel function of the first kind and $f_{\max}$ is the maximum Doppler frequency.

According to (1), the real part and the imaginary part of $H(f', t)$ are statistically independent Gaussian processes, each having the variance σ_0^2. Let us denote the envelope of the time-variant transfer function $H(f', t)$ at a specific carrier frequency $f' = f_0'$ as $\zeta(t) = |H(f_0', t)|$. The PDF of the envelope $\zeta(t)$ can be described by the Rayleigh distribution [9]

$$p_\zeta(r) = \begin{cases} \dfrac{r}{\sigma_0^2} e^{-\frac{r^2}{2\sigma_0^2}}, & r \geq 0, \\ 0, & r < 0. \end{cases} \quad (4)$$

B. Frequency-Selective SOC Channel Simulator

In this subsection, we design a frequency-selective channel simulator by making use of the SOC principle.

In the reference model described by (1), we replace the Gaussian processes $\mu_\ell(t)$ by stochastic complex processes $\hat{\mu}_\ell(t)$ ($\ell = 1, 2, \ldots, \mathcal{L}$), which can be represented by a sum of N_ℓ cisoids as follows [6]

$$\hat{\mu}_\ell(t) = \sum_{n=1}^{N_\ell} c_{n,\ell} e^{j(2\pi f_{n,\ell} t + \theta_{n,\ell})}, \quad (5)$$

where $c_{n,\ell}$, $f_{n,\ell}$, and $\theta_{n,\ell}$ represent the Doppler coefficient, the Doppler frequency, and the Doppler phase of the ℓth path, respectively. According to (5), the real part and the imaginary part of $\hat{\mu}_\ell(t)$ are correlated. However, such a correlation can be neglected under isotropic scattering conditions [6].

The Doppler phases $\theta_{n,\ell}$ are independent and identically distributed (i.i.d.) random variables, each having a uniform distribution over $[0, 2\pi)$. The Doppler coefficients $c_{n,\ell}$ and the Doppler frequencies $f_{n,\ell}$ are constant, which can be determined in such a way that the statistical properties of $\hat{\mu}_\ell(t)$ are as close as possible to those of the Gaussian random processes $\mu_\ell(t)$. In this paper, three parameter computation methods will be applied for computing the primary model parameters. Since most of the parameter design methods proposed for SOS models cannot directly be adopted to the SOC model, they need to be modified [10].

1) MEDS [11]: The parameters $c_{n,\ell}$ and $f_{n,\ell}$ can be determined by the MEDS as follows

$$c_{n,\ell} = \sigma_0 \sqrt{\frac{2}{N_\ell}}, \quad f_{n,\ell} = f_{\max} \sin\left[\frac{2\pi}{N_\ell}\left(n - \frac{1}{4}\right)\right]. \quad (6a,b)$$

2) R-MEDS: Performing the modification on the R-MEDS [12] results in the following equations

$$c_{n,\ell} = \sigma_0 \sqrt{\frac{2}{N_\ell}}, \quad f_{n,\ell} = f_{\max} \cos\left[\frac{2\pi}{N_\ell}\left(n - \frac{1}{4}\right) + \alpha_{n,\ell}\right], \quad (7a,b)$$

where the quantities $\alpha_{n,\ell}$ are i.i.d. random variables with a uniform distribution over $\left(-\frac{\pi}{2N_\ell}, \frac{\pi}{2N_\ell}\right]$.

3) MCM [13]: The application of the MCM allows us to compute the parameters $c_{n,\ell}$ and $f_{n,\ell}$ according to

$$c_{n,\ell} = \sigma_0 \sqrt{\frac{2}{N_\ell}}, \quad f_{n,\ell} = f_{\max} \sin(2\pi u_{n,\ell}), \quad (8a,b)$$

where $u_{n,\ell}$ are i.i.d. random variables uniformly distributed over the interval $(0, 1]$.

To guarantee the uncorrelated scattering (US) condition, the processes $\hat{\mu}_\ell(t)$ must be uncorrelated for different paths, i.e., for different values of ℓ. For the MEDS, the almost uncorrelatedness of the processes $\hat{\mu}_\ell(t)$ can be ensured by the convention $N_\ell = N + \ell - 1$, where N denotes the number of cisoids used in the first process $\hat{\mu}_1(t)$. Since the Doppler frequencies generated by the R-MEDS and the MCM are random variables, the uncorrelatedness is guaranteed even by using the same number of cisoids for different paths. In this paper, we assume that the number of cisoids belonging to different processes equals to N if the R-MEDS or the MCM is applied.

Similar to (1), we can express the time-variant transfer function $\hat{H}(f', t)$ of the stochastic SOC channel simulator as

$$\hat{H}(f', t) = \sum_{\ell=1}^{\mathcal{L}} a_\ell \hat{\mu}_\ell(t) e^{-j2\pi f' \tau_\ell'}, \quad (9)$$

which can be interpreted as a family of sample functions depending on the parameters $\theta_{n,\ell}$. If all phases $\theta_{n,\ell}$ are fixed, the stochastic process $\hat{\mu}_\ell(t)$ in (5) becomes a deterministic one. Hence, we obtain a single realization of $\hat{H}(f', t)$, which is also deterministic and can be used in simulations.

The mathematical description of the channel simulator allows us to study the temporal-frequency CF of the channel simulator. Due to the US condition, the temporal-frequency CF $\hat{r}_{HH}(v', \tau) = E\{\hat{H}^*(f', t)\hat{H}(f' + v', t + \tau)\}$ is given by [3]

$$\hat{r}_{HH}(v', \tau) = \sum_{\ell=1}^{\mathcal{L}} a_\ell^2 \hat{r}_{\mu_\ell \mu_\ell}(\tau) e^{-j2\pi v' \tau_\ell'}, \quad (10)$$

where $\hat{r}_{\mu_\ell \mu_\ell}(\tau) = \sum_{n=1}^{N_\ell} c_{n,\ell}^2 e^{j2\pi f_{n,\ell} \tau}$ describes the temporal ACF of the stochastic process $\hat{\mu}_\ell(t)$ [6].

The PDF $\hat{p}_\zeta(r)$ of the envelope $\hat{\zeta}(t) = |\hat{H}(f_0', t)|$ can be calculated similarly to [6]. According to Appendix A, we have

$$\hat{p}_\zeta(r) = (2\pi)^2 r \int_0^\infty \left[\prod_{\ell=1}^{\mathcal{L}} \prod_{n=1}^{N_\ell} J_0(2\pi a_\ell c_{n,\ell} y)\right] J_0(2\pi r y) y \, dy. \quad (11)$$

The envelope PDF $p_\zeta(r)$ of the reference channel model as well as the envelope PDF $\hat{p}_\zeta(r)$ of the SOC channel simulator designed by the MEDS with $\mathcal{L} = 6$ and $N = 6$ is depicted in Fig. 1. A good correspondence between the envelope PDFs of the reference model and that of the corresponding channel simulator can be observed. This figure shows also the simu-

2

lation results of the PDF of $\hat{\zeta}(t) = |\hat{H}(f'_0, t)|$ obtained from the simulation of $\hat{H}(f', t)$ given by (9) and averaging over 50 trials. Moreover, we prove in Appendix B that $\hat{p}_\zeta(r) \to p_\zeta(r)$ for $N_\ell \to \infty$.

III. PERFORMANCE OF THE SOC CHANNEL SIMULATOR IN COHERENT DPSK OFDM SYSTEMS

Section III analyzes the performance of the wideband SOC channel simulator in a coherent DPSK OFDM system.

For the reference channel model, it is shown in Section II that the absolute value of the time-variant transfer function follows the Rayleigh distribution. Therefore, the reference BEP is given by [9]

$$P_b = \frac{1}{2(1 + \overline{\gamma}_b)}, \tag{12}$$

where $\overline{\gamma}_b = 2\sigma_0^2 E_b/N_0$ is the average signal-to-noise ratio.

The BEP of the simulation system $\hat{P}_b$ can be calculated by the relation

$$\hat{P}_b = \int_0^\infty P_{b|r}(r)\hat{p}_\zeta(r)dr, \tag{13}$$

where

$$P_{b|r}(r) = \frac{1}{2}e^{-r^2 \frac{E_b}{N_0}}, \tag{14}$$

is the conditional BEP of the coherent DPSK system [9].

If we substitute (11) and (14) in (13), we obtain the following analytical expression for the BEP of the DPSK OFDM system using the SOC channel simulator

$$\hat{P}_b = \frac{\pi^2}{E_b/N_0}\int_0^\infty e^{-\frac{\pi^2 y^2}{E_b/N_0}}\left[\prod_{\ell=1}^{\mathcal{L}}\prod_{n=1}^{N_\ell} J_0(2\pi a_\ell c_{n,\ell}y)\right] y\, dy. \tag{15}$$

The derivation of the BEP $\hat{P}_b$ can be found in Appendix C. Note that the BEP $\hat{P}_b$ is independent of the Doppler frequencies $f_{n,\ell}$. The channel simulators designed with the MEDS, the R-MEDS, and the MCM are equivalent w.r.t. the BEP, since the Doppler coefficients $c_{n,\ell}$ calculated by these three methods are the same.

The BEP P_b computed according to (12) is presented in Fig. 2. This figure also illustrates the BEP performance of the coherent DPSK OFDM system using different SOC channel simulators designed with the MEDS, the R-MEDS, and the MCM. The theoretical results are validated by simulations.
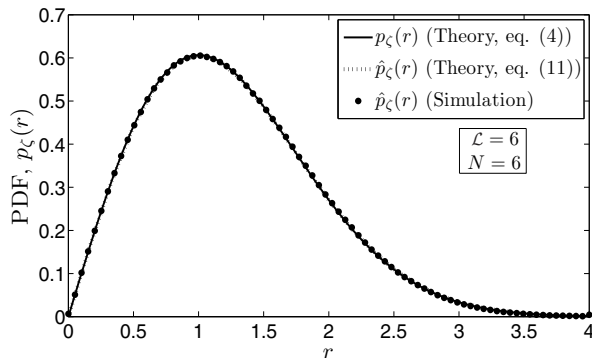
Fig. 1. Probability density function $p_\zeta(r)$ of the absolute value of the time-variant transfer function $\zeta(t) = |H(f'_0, t)|$.
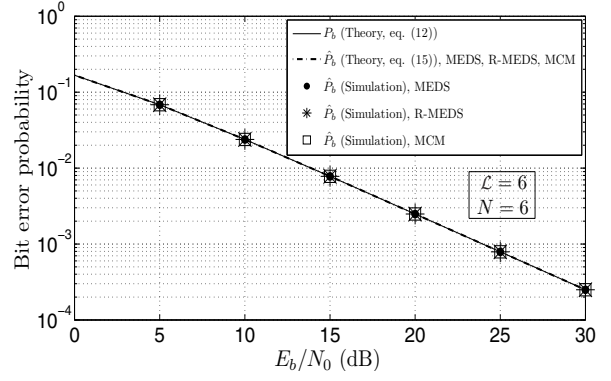
Fig. 2. Coherent DPSK OFDM system performance using the reference model and the SOC channel simulators designed with the MEDS, the R-MEDS, and the MCM.

In all simulations, we use the 6-path channel model with the propagation delays $\tau'_\ell \in \{0, 100, 200, 300, 400, 500\}\,\mu s$ ($\ell = 1, 2, \ldots, \mathcal{L}$). The powers assigned to the 6 different paths equal to $\{0, -4, -8, -12, -16, -20\}\,$dB. We consider the DPSK OFDM system consisting of $K = 128$ subcarriers with a sampling duration of $T = 100\,\mu s$.

We also prove in Appendix C that $\hat{P}_b \to P_b$ holds as $N_\ell \to \infty$. However, the deviation of the BEP between $\hat{P}_b$ and P_b cannot be ignored if the number of cisoids is small. Here, we introduce the relative error of the BEP $\hat{P}_b$

$$\varepsilon_{BEP} = \frac{\hat{P}_b - P_b}{P_b} \tag{16}$$

to evaluate the BEP deviation in terms of N.

The influence of the number of cisoids N on the relative error is illustrated in Fig. 3. From this figure, we can conclude that the absolute value of the relative error $|\varepsilon_{BEP}|$ is less than 4.327% if $N \geq 5$.

IV. PERFORMANCE OF THE SOC CHANNEL SIMULATOR IN NONCOHERENT DPSK OFDM SYSTEMS

According to [14, pp. 193], the BEP of noncoherent DPSK in Rayleigh fading is given by

$$P_b = \frac{1}{2}\left[1 - \frac{r_{hh}(T)}{1 + \frac{1}{\overline{\gamma}_b}}\right], \tag{17}$$

where $r_{hh}(T)$ denotes the value of the temporal ACF $r_{hh}(\tau) = \sum_{\ell=1}^{\mathcal{L}} a_\ell^2 r_{\mu_\ell\mu_\ell}(\tau)$ of the channel impulse response
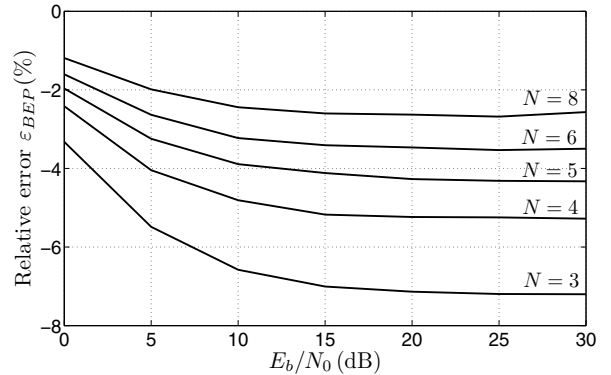
Fig. 3. Evaluation of the relative error of the BEP ε_{BEP} for the coherent DPSK OFDM system for various values of the number of cisoids N.

3

at $\tau = T$. Different from [14], the channel response in this paper is described by a time-variant transfer function. Thus, we can express the BEP of a noncoherent DPSK OFDM system by replacing $r_{hh}(T)$ in (17) with the temporal-frequency CF $r_{HH}(v',\tau)$ at $v' = f_s$ and $\tau = T$, i.e.,

$$P_b = \frac{1}{2}\left[1 - \frac{r_{HH}(f_s,T)}{1 + \frac{1}{\bar{\gamma}_b}}\right]. \qquad (18)$$

Here $f_s = 1/(KT)$ is the subcarrier spacing. Substituting $r_{HH}(v',\tau)$ given by (2) in (18), we have

$$P_b = \frac{1}{2}\left[1 - \frac{2\sigma_0^2 J_0(2\pi f_{\max}T)\sum\limits_{\ell=1}^{\mathcal{L}} a_\ell^2 e^{-j2\pi f_s \tau_\ell'}}{1 + \frac{1}{\bar{\gamma}_b}}\right]. \qquad (19)$$

Assuming that the PDF $\hat{p}_\zeta(r)$ is close to the PDF $p_\zeta(r)$ of the reference channel model, the BEP of the simulation system $\hat{P}_b$ for the DPSK OFDM system employing the wideband SOC channel simulator is similar to the expression in (18). We only need to replace $r_{HH}(f_s,T)$ in (18) by $\hat{r}_{HH}(v',\tau)$ at $v' = f_s$ and $\tau = T$ [see eq. (10)]. Thus, we finally obtain

$$\hat{P}_b \approx \frac{1}{2}\left[1 - \frac{\sum\limits_{\ell=1}^{\mathcal{L}} a_\ell^2 e^{-j2\pi f_s \tau_\ell'} \sum\limits_{n=1}^{N_\ell} c_{n,\ell}^2 e^{j2\pi f_{n,\ell}T}}{1 + \frac{1}{\bar{\gamma}_b}}\right]. \qquad (20)$$

Using the relative error ε_{BEP} in (16) as a criterion, we can now evaluate the performance of the MEDS, the R-MEDS, and the MCM. In this paper, the inequality $f_{n,\ell}T \ll 1$ holds. According to the approximation $e^x \approx 1 + x + x^2/2\,(x \ll 1)$, the temporal ACF $\hat{r}_{\mu_\ell \mu_\ell}(T) = \sum_{n=1}^{N_\ell} c_{n,\ell}^2 e^{j2\pi f_{n,\ell}T}$ can be approximated as follows

$$\hat{r}_{\mu_\ell \mu_\ell}(T) \approx \sum_{n=1}^{N_\ell} c_{n,\ell}^2 [1 + j2\pi f_{n,\ell}T - 2(\pi f_{n,\ell}T)^2]$$
$$= \hat{r}_{\mu_\ell \mu_\ell}(0) + T\dot{\hat{r}}_{\mu_\ell \mu_\ell}(0) + \frac{T^2}{2}\ddot{\hat{r}}_{\mu_\ell \mu_\ell}(0). \qquad (21)$$

Here, $\dot{\hat{r}}_{\mu_\ell \mu_\ell}(\cdot)$ and $\ddot{\hat{r}}_{\mu_\ell \mu_\ell}(\cdot)$ denote the derivative and the second derivative of $\hat{r}_{\mu_\ell \mu_\ell}(\cdot)$, respectively.

For the special case, where the power spectral density (PSD) is symmetrical, the value for the imaginary part of $\hat{r}_{\mu_\ell \mu_\ell}(T)$ is zero. Since the power constraint $\hat{r}_{\mu_\ell \mu_\ell}(0) = r_{\mu_\ell \mu_\ell}(0)$ holds for all the three methods mentioned above, we make a further simplification concerning (21) [4]

$$\hat{r}_{\mu_\ell \mu_\ell}(T) \approx \hat{r}_{\mu_\ell \mu_\ell}(0) + \frac{T^2}{2}\ddot{\hat{r}}_{\mu_\ell \mu_\ell}(0)$$
$$= r_{\mu_\ell \mu_\ell}(0) + \frac{T^2}{2}\ddot{r}_{\mu_\ell \mu_\ell}(0) - \frac{T^2}{2}\triangle\beta_\ell$$
$$= r_{\mu_\ell \mu_\ell}(T) - \frac{T^2}{2}\triangle\beta_\ell. \qquad (22)$$

In the preceding equation, $\triangle\beta_\ell = \ddot{r}_{\mu_\ell \mu_\ell}(0) - \ddot{\hat{r}}_{\mu_\ell \mu_\ell}(0)$ represents the model error of the SOC channel simulator. For the Jakes PSD, we have $\beta_\ell = -\ddot{r}_{\mu_\ell \mu_\ell}(0) = (2\pi\sigma_0 f_{\max})^2$ for the

reference channel model and for the SOC channel simulator, we obtain $\ddot{\hat{r}}_{\mu_\ell \mu_\ell}(0) = -(2\pi)^2 \sum_{n=1}^{N_\ell}(c_{n,\ell}f_{n,\ell})$.

By making use of (2), (10), and (22), we can rewrite the temporal-frequency CF $\hat{r}_{HH}(f_s,T)$ in (10) as follows

$$\hat{r}_{HH}(f_s,T) \approx r_{HH}(f_s,T) - \frac{T^2}{2}\sum_{n=1}^{N_\ell} a_\ell^2 \triangle\beta_\ell e^{-j2\pi f_s \tau_\ell'}. \quad (23)$$

Putting (23) into (20) and taking the relation (19) into consideration, the BEP $\hat{P}_b$ can be expressed in closed-form as

$$\hat{P}_b = P_b + \triangle P_b, \qquad (24)$$

where

$$\triangle P_b = \frac{\left(\frac{T}{2}\right)^2 \sum\limits_{\ell=1}^{\mathcal{L}} a_\ell^2 \triangle\beta_\ell e^{-j2\pi f_s \tau_\ell'}}{1 + \frac{1}{\bar{\gamma}_b}}. \qquad (25)$$

By making use of (25), we can express the relative error of the BEP as follows

$$\varepsilon_{BEP} = \frac{\frac{T^2}{2}\sum\limits_{\ell=1}^{\mathcal{L}} a_\ell^2 \triangle\beta_\ell e^{-j2\pi f_s \tau_\ell'}}{1 + \frac{1}{\bar{\gamma}_b} - 2\sigma_0^2 J_0(2\pi f_{\max}T)\sum\limits_{\ell=1}^{\mathcal{L}} a_\ell^2 e^{-j2\pi f_s \tau_\ell'}}. \quad (26)$$

Since the model error $\triangle\beta_\ell = 0$ if the MEDS is applied [3], it follows that the relative error $\varepsilon_{BEP} = 0$. Thus, we can say that the SOC channel simulator designed with the MEDS is equivalent to the reference channel model in terms of the BEP. The analytical results for the BEP P_b and $\hat{P}_b$ are depicted in Fig. 4 for different maximum Doppler frequencies. This figure also shows the relevant simulation results, which match the analytical results very well. All parameters are identical to the parameters used in Section III.

When designing the SOC channel simulator by the R-MEDS, we find the expected value $E\{\triangle\beta_\ell\}$ of the model error $\triangle\beta_\ell$ equals to 0 and the variance $\mathrm{Var}\{\triangle\beta_\ell\}$ is $\beta_\ell^2/(4N_\ell^2)$. For the MCM, the model error $\triangle\beta_\ell$ is approximately normally distributed, i.e., $\triangle\beta_\ell \sim N(0, \beta_\ell^2/(2N_\ell))$ [3]. The BEP performances of the noncoherent DPSK OFDM system using the channel simulator designed with the R-MEDS and the MCM are shown in Fig. 5 and Fig. 6 (4 realizations of the BEP $\hat{P}_b$ without averaging), respectively. For comparison, we replot in
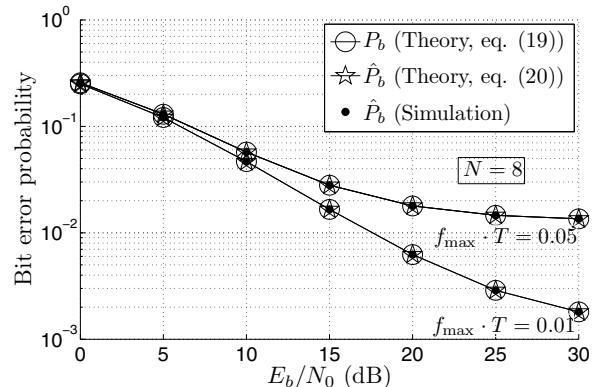

Fig. 4. Noncoherent DPSK OFDM system performance using the reference model and the SOC channel simulator designed with the MEDS.

these two figures the BEP P_b computed according to (19). From these figures, it can be seen that the single realization of the BEP, denoted by $\tilde{P}_b$, deviates from P_b in a random manner. The reason is that the R-MEDS and the MCM are typical stochastic parameter design methods. Different from the MEDS, the discrete Doppler frequencies generated by these two methods are random variables. It can be observed that the BEP degrades if the maximum Doppler frequency f_{max} changes from 100 Hz to 500 Hz. The approximation $\tilde{P}_b \approx P_b$ is good when using the R-MEDS. However, comparing Fig. 5 and Fig. 6, we find that the deviation between $\tilde{P}_b$ and P_b in Fig. 6 is large and cannot be neglected. The reason for this observation is that the variance of the model error using the MCM is larger than that of using the R-MEDS. Therefore, averaging over the BEP $\tilde{P}_b$ obtained from different realizations is unavoidable if the MCM is used.

V. Conclusion

In this paper, the performance of the frequency-selective reference channel model and the corresponding SOC channel simulator have been analyzed w.r.t. the BEP of DPSK OFDM systems. Analytical expressions for the BEP have been derived for both the coherent and noncoherent DPSK OFDM systems. From the derivations of the BEP, the relative error of the BEP has been studied, which allows to reduce the channel
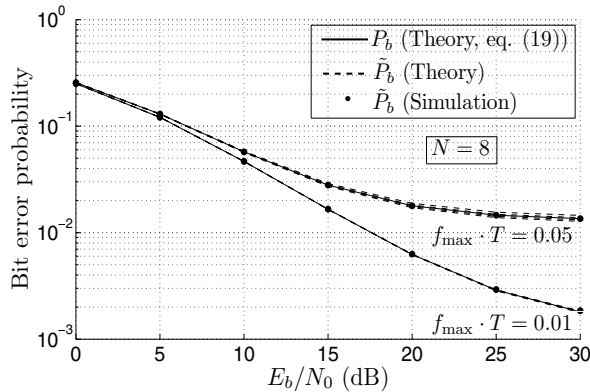

Fig. 5. Noncoherent DPSK OFDM system performance using the reference model and the SOC channel simulator designed with the R-MEDS ($\tilde{P}_b$: realizations of $\hat{P}_b$ in (20)).
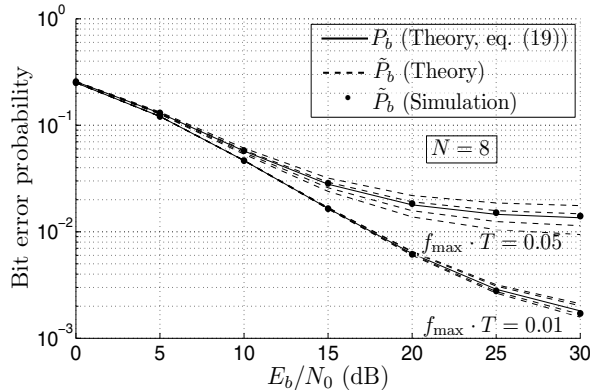

Fig. 6. Noncoherent DPSK OFDM system performance using the reference model and the SOC channel simulator designed with the MCM ($\tilde{P}_b$: realizations of $\hat{P}_b$ in (20)).

realization expenditure to a lower bound without causing any obvious BEP distortion. We have compared the best deterministic parameter design method (MEDS), the best stochastic one (R-MEDS), and the MCM by employing the relative error of the BEP as an appropriate criterion.

For coherent DPSK OFDM systems, it is shown by theory and confirmed by simulations that the SOC channel simulators designed by the MEDS, the R-MEDS, and the MCM are equivalent w.r.t. the BEP performance. When the number of cisoids tends to infinity, it has been proved that the BEP of the simulation system in the presence of a wideband SOC channel simulator converges to the reference BEP. The relative error of the BEP can be neglected if the channel simulator is designed using not less than 5 cisoids. For noncoherent DPSK OFDM systems, a closed-form expression has been derived for the relative error, which provides a powerful tool when discussing the performance of different parameter computation methods. From our results, we can conclude that the performance of the MEDS and the R-MEDS is almost the same w.r.t. the relative error of the BEP. However, both methods outperform the MCM.

APPENDIX A
DERIVATION OF THE ENVELOPE PDF $\hat{p}_\zeta(r)$

This appendix is devoted to the derivation of the PDF of the envelope $\hat{\zeta}(t) = |\hat{H}(f_0', t)|$. Suppose that $\hat{H}_{1,\ell}(f_0', t)$ and $\hat{H}_{2,\ell}(f_0', t)$ represent the real part and the imaginary part of the ℓth component $a_\ell \hat{\mu}_\ell(t) e^{-j2\pi f_0' \tau_\ell'}$ of $H(f_0', t)$, respectively. For fixed values of $t = t_0$, the joint characteristic function $\hat{\Psi}_{H_{1,\ell} H_{2,\ell}}(\nu_1, \nu_2)$ of $\hat{H}_{1,\ell}(f_0', t_0)$ and $\hat{H}_{2,\ell}(f_0', t_0)$ can be expressed by the relation [6]

$$\hat{\Psi}_{H_{1,\ell} H_{2,\ell}}(\nu_1, \nu_2) = \prod_{n=1}^{N_\ell} J_0(2\pi a_\ell c_{n,\ell} \sqrt{\nu_1^2 + \nu_2^2}). \quad \text{(A.1)}$$

We denote the real and imaginary parts of $H(f', t)$ by $H_1(f', t)$ and $H_2(f', t)$, respectively. As mentioned before, the Doppler phases θ_n are i.i.d. random variables, which leads to the fact that the terms $\hat{H}_i(f_0', t_0) = \hat{H}_{i,1}(f_0', t_0) + \hat{H}_{i,2}(f_0', t_0) + \cdots + \hat{H}_{i,\mathcal{L}}(f_0', t_0)$ are also i.i.d. random variables ($i = 1, 2$). Thus, the joint characteristic function $\hat{\Psi}_{H_1 H_2}(\nu_1, \nu_2)$ of $\hat{H}_1(f_0', t_0)$ and $\hat{H}_2(f_0', t_0)$ can be formulated as the $\mathcal{L}$-fold product of the joint characteristic functions $\hat{\Psi}_{H_{1,\ell} H_{2,\ell}}(\nu_1, \nu_2)$, i.e.,

$$\hat{\Psi}_{H_1 H_2}(\nu_1, \nu_2) = \prod_{\ell=1}^{\mathcal{L}} \prod_{n=1}^{N_\ell} J_0(2\pi a_\ell c_{n,\ell} \sqrt{\nu_1^2 + \nu_2^2}). \quad \text{(A.2)}$$

Then, the joint PDF $\hat{p}_{H_1 H_2}(x_1, x_2)$ is given by the inverse Fourier transform of $\hat{\Psi}_{H_{1,\ell} H_{2,\ell}}(\nu_1, \nu_2)$ [15, eq. (3.397-1,2)]

$$\hat{p}_{H_1 H_2}(x_1, x_2) = \int_{-\infty}^{\infty} \hat{\Psi}_{H_1 H_2}(\nu_1, \nu_2) e^{j2\pi(\nu_1 x_1 + \nu_2 x_2)} d\nu_1 d\nu_2$$

$$= 2\pi \int_0^\infty \left[\prod_{\ell=1}^{\mathcal{L}} \prod_{n=1}^{N_\ell} J_0(2\pi a_\ell c_{n,\ell} y) \right]$$

$$\cdot J_0(2\pi y \sqrt{x_1^2 + x_2^2}) \, y \, dy. \quad \text{(A.3)}$$

5

The transformation of the Cartesian coordinates (x_1, x_2) into polar coordinates (r, θ) with $x_1 = r\cos\theta$ and $x_2 = r\sin\theta$ allows us to calculate the joint PDF $\hat{p}_{\zeta\vartheta}(r, \theta)$ of the envelope $\hat{\zeta}(t) = |\hat{H}(f_0', t)|$ and the phase $\hat{\vartheta}(t) = \arg\{\hat{H}(f_0', t)\}$ as follows

$$\hat{p}_{\zeta\vartheta}(r, \theta) = r\,\hat{p}_{H_1 H_2}(r\cos\theta, r\sin\theta) \tag{A.4}$$

$$= 2\pi r \int_0^\infty \left[\prod_{\ell=1}^{\mathcal{L}} \prod_{n=1}^{N_\ell} J_0(2\pi a_\ell c_{n,\ell} y) \right] \cdot J_0(2\pi r y)\, y\, dy,$$

for $z \geq 0$ and $|\theta| \leq \pi$. Integrating the joint PDF $\hat{p}_{\zeta\vartheta}(r, \theta)$ over θ results in

$$\hat{p}_\zeta(r) = (2\pi)^2 r \int_0^\infty \left[\prod_{\ell=1}^{\mathcal{L}} \prod_{n=1}^{N_\ell} J_0(2\pi a_\ell c_{n,\ell} y) \right] \cdot J_0(2\pi r y)\, y\, dy. \tag{A.5}$$

APPENDIX B
PROOF OF $\hat{p}_\zeta(r) \to p_\zeta(r)$ HOLDS IF $N_\ell \to \infty$

In the following, we prove that the envelope PDF $\hat{p}_\zeta(r)$ of the SOC channel simulator converges to the Rayleigh distribution as $N_\ell \to \infty$. According to [3, p. 335], we have

$$\lim_{N_\ell \to \infty} \prod_{n=1}^{N_\ell} J_0(2\pi a_\ell c_{n,\ell} y) = e^{-2(\pi a_\ell \sigma_0 y)^2}. \tag{B.1}$$

By using the result in (B.1) and considering the relation $\sum_{\ell=1}^{\mathcal{L}} a_\ell^2 = 1$, we obtain

$$\prod_{\ell=1}^{\mathcal{L}} \prod_{n=1}^{N_\ell} J_0(2\pi a_\ell c_{n,\ell} y) = e^{-2(\pi\sigma_0 y)^2 \sum_{\ell=1}^{\mathcal{L}} a_\ell^2} = e^{-2(\pi\sigma_0 y)^2} \tag{B.2}$$

as $N_\ell \to \infty$. Thus, in the limit $N_\ell \to \infty$, the envelope PDF $\hat{p}_\zeta(r)$ in (A.5) tends to

$$\hat{p}_\zeta(r) = (2\pi)^2 r \int_0^\infty e^{-2(\pi y \sigma_0)^2} \cdot J_0(2\pi r y)\, y\, dy$$

$$= \frac{r}{\sigma_0^2} e^{-\frac{r^2}{2\sigma_0^2}}, \quad r \geq 0, \tag{B.3}$$

which is known as the Rayleigh distribution.

APPENDIX C
DERIVATION OF THE BEP $\hat{P}_b$

Putting (11) and (14) into (13) results in the following twofold integral for the BEP

$$\hat{P}_b = 2\pi^2 \int_0^\infty \int_0^\infty r e^{-r^2 \frac{E_b}{N_0}} J_0(2\pi r y) dr$$

$$\cdot \left[\prod_{\ell=1}^{\mathcal{L}} \prod_{n=1}^{N_\ell} J_0(2\pi a_\ell c_{n,\ell} y) \right] y\, dy. \tag{C.1}$$

The integral over r can be solved by using the relation [15, eq. (6.631.4)]

$$\int_0^\infty r e^{-\alpha r^2} J_0(\beta r) dr = \frac{e^{-\frac{\beta^2}{4\alpha}}}{2\alpha}, \quad \text{Re}\{\alpha\} > 0, \beta > 0. \tag{C.2}$$

After some calculations, we finally obtain

$$\hat{P}_b = \frac{\pi^2}{E_b/N_0} \int_0^\infty e^{-\frac{\pi^2 y^2}{E_b/N_0}} \left[\prod_{\ell=1}^{\mathcal{L}} \prod_{n=1}^{N_\ell} J_0(2\pi a_\ell c_{n,\ell} y) \right] y\, dy. \tag{C.3}$$

Next, we prove that $\hat{P}_b \to P_b$ holds if $N_\ell \to \infty$. If we substitute the result in (B.2) into the right-hand side of (B.3), we obtain

$$\hat{P}_b = \frac{\pi^2}{E_b/N_0} \int_0^\infty e^{-\frac{\pi^2 y^2}{E_b/N_0}} e^{-2(\pi\sigma_0 y)^2} y\, dy$$

$$= \frac{1}{2(1 + 2\sigma_0^2 \frac{E_b}{N_0})}$$

$$= \frac{1}{2(1 + \overline{\gamma}_b)} \tag{C.4}$$

as $N_\ell \to \infty$.

REFERENCES

[1] S. O. Rice, "Mathematical analysis of random noise," *Bell Syst. Tech. J.*, vol. 23, pp. 282–332, Jul. 1944.
[2] ——, "Mathematical analysis of random noise," *Bell Syst. Tech. J.*, vol. 24, pp. 46–156, Jan. 1945.
[3] M. Pätzold, *Mobile Fading Channels*. Chichester: John Wiley & Sons, 2002.
[4] M. Pätzold and F. Laue, "The performance of deterministic Rayleigh fading channel simulators with respect to the bit error probability," in *Proc. 51th Vehicular Technology Conference, VTC 2000-Spring*. Tokyo, Japan, May 2000, pp. 1998–2003.
[5] Y. Ma and M. Pätzold, "Wideband two-ring MIMO channel models for mobile-to-mobile communications," in *Proc. 10th International Symposium on Wireless Personal Multimedia Communications, WPMC 2007*. Jaipur, India, Dec. 2007, pp. 380–384.
[6] M. Pätzold and B. Talha, "On the statistical properties of sum-of-cisoids-based mobile radio channel models," in *Proc. 10th International Symposium on Wireless Personal Multimedia Communications, WPMC 2007*. Jaipur, India, Dec. 2007, pp. 394–400.
[7] P. A. Bello, "Characterization of randomly time-variant linear channels," *IEEE Trans. Commun. Syst.*, vol. 11, no. 4, pp. 360–393, Dec. 1963.
[8] M. Pätzold, "System function and characteristic quantities of spatial deterministic Gaussian uncorrelated scattering processes," in *Proc. 57th Vehicular Technology Conference, VTC 2003-Spring*. Jeju, Korea, Apr. 2003, pp. 256–261.
[9] J. Proakis and S. Massoud, *Digital Communications*. New York: McGraw-Hill, 5th edition, 2007.
[10] C. A. Gutiérrez and M. Pätzold, "Sum-of-sinusoids-based simulation of flat fading wireless propagation channels under non-isotropic scattering conditions," in *Proc. 50th IEEE Global Communication Conference, GLOBECOM 2007*. Washington, D.C., USA, Nov. 2007, pp. 3842–3846.
[11] M. Pätzold and C. A. Gutiérrez, "Level-crossing rate and average duration of fades of the envelope of a sum-of-cisoids," in *Proc. 67th IEEE Vehicular Technology Conference, VTC2008-Spring*. Singapore, May 2008, pp. 488–494.
[12] Y. R. Zheng and C. Xiao, "Simulation models with correct statistical properties for Rayleigh fading channels," *IEEE Trans. Commun.*, vol. 51, no. 6, pp. 920–928, Jun. 2003.
[13] P. Höher, "A statistical discrete-time model for the WSSUS multipath channel," *IEEE Trans. Veh. Technol.*, vol. VT–41, no. 4, pp. 461–468, Nov. 1992.
[14] A. Goldsmith, *Wireless Communications*. Cambridge University Press, 2005.
[15] I. S. Gradshteyn and I. M. Ryzhik, *Tables of Integrals, Series, and Products*. Academic Press, 6th edition, 2000.

6